

Monomer diffusion rates in photopolymer material. Part II. High-frequency gratings and bulk diffusion

C. E. Close,¹ M. R. Gleeson,¹ D. A. Mooney,² and J. T. Sheridan^{1,*}

¹Communications and Optoelectronic Research Centre, SFI Strategic Research Centre in Solar Energy Conversion, School of Electrical, Electronic and Communications Engineering, University College Dublin, Belfield, Dublin 4, Ireland

²School of Chemical and Bioprocess Engineering, College of Engineering, Mathematical and Physical Sciences, University College Dublin, Belfield, Dublin 4, Ireland

*Corresponding author: john.sheridan@ucd.ie

Received October 25, 2010; revised December 21, 2010; accepted January 16, 2011;
posted January 25, 2011 (Doc. ID 137126); published March 23, 2011

Photosensitive polymers are of practical importance, and mass transport within such materials plays a critical role in their behavior. Building on the work in Part I [J. Opt. Soc. Am. B doc. ID 136413 (posted 5 January 2011, in press)], the diffusion constants of a number of materials (i.e., acrylamide, polyacrylamide, water, propanol, and acetone) within a photosensitive layer are measured. A combination of optical and physical chemistry techniques is applied under different conditions. Determining the rates of diffusion is beneficial as it: (i) indicates material stability over time and (ii) supports material characterization, modeling, and performance optimization. © 2011 Optical Society of America

OCIS codes: 090.0090, 050.2770, 050.7330, 160.5470, 090.2900.

1. INTRODUCTION

As discussed in Part I [1], there is much confusion in the literature regarding the value of the rate of diffusion of an acrylamide (AA) monomer in a polyvinylalcohol (PVA)-based holographic material. Estimates ranging from 10^{-7} to 10^{-14} cm²/s have been reported by different groups (see [2–7]). The many applications of such free-radical photopolymer materials [8–13] make understanding the material photo-kinetics very important. The material behavior appears to be best described using diffusion-based models, i.e., the nonlocal polymerization-driven diffusion (NPDD) model [2,14–16]. In this model, it is assumed that, because of crosslinking, only monomer diffusion is significant postexposure.

In Part I [1], the rate of diffusion of monomer in an AA/PVA material, D_{AA} , was determined based on experiments involving large-period gratings. The results indicated a maximum value of $D_{AA} \sim 10^{-9}$ cm²/s [1], however, the actual value is slower due to the continuing optical effects of surface relief profile evolution during measurement. In this paper, we proceed to further study the upper (fastest) and lower (slowest) diffusion rates possible using other experimental methods.

First, we perform experiments to determine a lower bound for D_{AA} . This is done by studying the rate of diffusion of polyacrylamide (PA) in AA/PVA material with varying amounts of the crosslinker, using holographic techniques and long continuous exposures. AA will diffuse more rapidly than the larger, more complex PA, i.e., $D_{AA} > D_{PA}$. We note that, in the absence of a crosslinker, higher average values of D_{PA} are found, indicating the presence of lower-energy diffusion pathways. It is noted that more rapid grating strength decays, indicating higher rates of diffusion, are observed immediately postexposure. For these high spatial frequency exposures, the effects of surface relief gratings can be neglected (see [1]).

Continuing our study of diffusion of PA in the layer, we note that, for shorter exposures, less PA is formed. When no cross-

linker is included, relaxation postexposure will involve simultaneous PA and AA counterdiffusion, both of which act to reduce grating strength. Therefore, in this situation, calculating a single effective modulation rate of diffusion, D_M , using the method described in Subsection 4.C in Part I [1], yields a D_M value that, for decreasing exposure times, approaches that of D_{AA} from below.

In order to find a value for the upper bound, i.e., the largest possible value of D_{AA} , we then examine the rate of diffusion of smaller molecules in the layer. The materials chosen are water, propanol, and acetone. These materials were selected because they are all liquids at room temperature and have smaller molecular weights and lower dipole moments than AA. Furthermore, two of them are hydrocarbon materials with similar radii. Given these facts, which suggest a lower interaction with the host material, it would seem reasonable that they would diffuse more quickly through the layer than the heavier AA, which is a solid at room temperature.

The paper is organized as follows: in Section 2, the rate of diffusion of the PA formed during photopolymerization is determined using holographic techniques. Then, in Section 3, the rates of diffusion of water, propanol, and acetone in the material layer are investigated using a standard weight-based technique. Experimental results are presented and compared in Section 4. Section 5 contains some concluding remarks.

2. DIFFUSION OF PA POSTEXPOSURE USING HOLOGRAPHIC TECHNIQUES

In this section, we determine the diffusion of PA in the layer by monitoring the degradation of a recorded holographic grating postexposure. In Subsection 2.A, the material composition is briefly described. In Subsection 2.B, the analysis used to find the value of the diffusion constant, given the measured reduction of the diffracted probe beam intensity with time, is discussed. In Subsection 2.C, the experimental method and

setup used are discussed. Finally, in Subsection 2.D, the experiment to examine short exposures is discussed.

A. Material Chemical Composition: the Role of Crosslinker

As discussed, the material used is an AA/PVA dry layer, where the PVA has a molecular weight in the range 30,000–70,000 u [1]. When examining the diffusion of the PA, however, different amounts of bisacrylamide (BA) are used, as described in Subsection 2.B. The BA is a crosslinking agent, the inclusion of which acts to create a more complex PA structure during polymerization. Reducing the quantity of BA in the material results in a reduction in the complexity of the polymerized material [17]. Therefore, as the concentration of BA decreases, the mean value (D_{PA}) will increase and, while it is expected to always be smaller than D_{AA} , it will increase approaching the D_{AA} value from below.

B. Longer Exposures and Varying Crosslinker Quantities

The rate of diffusion of the PA in the layer is found indirectly using optical techniques similar to those used in Part I [1]. A diffraction grating is formed by exposing the material to a sinusoidal interference pattern with a spatial frequency of 1000 lines/mm. Thus, we are operating in the Bragg regime rather than the Raman–Nath regime [1]. A long duration exposure is performed in order to use up most of the monomer in the layer. As in Part I, the diffraction efficiency, η , of the grating is monitored postexposure using a probe beam to which the dye is insensitive [1,18]. The strength of the grating gradually decays as a result of diffusion of the PA within the layer and, from this, the rate of diffusion is found. The quantity of BA in the material was varied between experiments to demonstrate its effect on the rate of monomer diffusion. In the absence of BA, the resulting PA is not crosslinked and can diffuse more easily within the layer, with the result that the recorded sinusoidal PA density distribution decays with time.

Using the resulting measured diffraction efficiency data, the rate of diffusion is found. In what follows, we proceed using the diffusion model as described in [1,19], and the experimental method described in Subsection 2.C in Part I. Spatial concentration distributions of PA and AA exist in the material following exposure, and both undergo diffusion [14]. The effect of the AA diffusion is limited, as much of it is used up during the long exposures. Furthermore, assuming that the diffusion of the AA takes place over a much shorter time frame than that of the PA chains, the long-term effect of AA diffusion on the grating strength postexposure can be assumed to be negligible and can therefore be omitted from the analysis. This assumption can be justified because (1) the molecular weight of the AA monomer is significantly lower than that of the PA chains, and (2) the PA chains have complex structures compared to the AA molecule. Thus, the PA chains will find it more difficult to move in the dry layer and, hence, will have a rate of diffusion much lower than that of the AA (i.e., the effects associated with PA diffusion are observed to take place over a much longer time frame). We note that a more complete analysis of the evolution of the grating modulation requires the use of the Lorentz–Lorenz relation [14,20]. Furthermore, we note that the PA, produced by photopolymerization, will in fact have a distribution of molecular

weights and diffusion rates; such distribution effects are neglected in the analysis.

C. Experimental Method for Determining D_{PA}

An optical system, similar to that illustrated in Part I [1,19], is used to record and probe the gratings. The effect of mechanical vibrations is minimized using a floating optical table. As the light passes through the material, the dye undergoes an oxidation reaction and adsorbs a photon in the presence of the electron donor, which then produces free radicals. Polymerization of the AA is caused by these free radicals and results in the formation and growth (propagation) of PA chains [15]. The resulting PA spatial distribution gives rise to a volume refractive index variation and, in the case of illumination by a sinusoidal interference pattern, the recording of a periodic grating.

Probing the grating, the beam diffraction intensity evolution is measured over time and used to calculate the diffraction efficiency, η and, thus, the grating strength using Kogelnik's coupled wave theory [21]. From the diffracted probe beam intensity data obtained postexposure, the PA grating refractive index modulation amplitude can be extracted, and, hence, the diffusion coefficient can be estimated using Eq. (19) in Part I, where, in this case, D_M is approximately equivalent to D_{PA} . The experimental results for D_{PA} are presented and discussed in Section 4.

From these long exposure results it can be seen (in particular in the cases without a crosslinker present) that, in the initial period postexposure, the grating decays at a faster rate than later due to rapid diffusion of the remaining AA. During the recording of weak/short exposures, less PA is formed and the decay of the grating, and, hence, the diffusion rate, will be more influenced by AA diffusion. Therefore, we examine this weak exposure situation, focusing on the initial period postexposure.

D. Short Exposures without a Crosslinker

A typical example of grating diffraction efficiency evolution for a longer exposure, using the material discussed in Subsection 2.A, i.e., without a crosslinker, is shown in Fig. 1. The vertical y -axis range is chosen to emphasize the η values of interest. Examining the curve, it is clear that, postexposure, the grating continues to evolve for a considerable period of time. For the instance shown in Fig. 1, the grating reaches a peak diffraction efficiency of $\eta \sim 22\%$. The exposing pattern is then switched off and, almost immediately, the grating starts to decay [14]. We see that $\sim 50\%$ of the total decrease

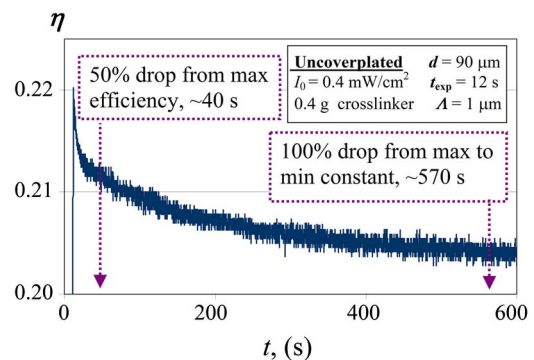


Fig. 1. (Color online) Evolution of grating diffraction efficiency illustrating the decay of the grating strength postexposure.

takes place in the first 30 s postexposure. A further ~ 530 s are required for the grating strength to decay to its final constant value. Clearly, the grating decay has less of an impact on the grating strength over time [22]. As noted, such postexposure decay is primarily due to a combination of diffusion processes, i.e., D_{AA} , D_{PA} , and the diffusion of water out of/into the layer [1,14,23,24].

Short exposures are carried out with the evolution of the grating strength being monitored for up to 60 s postexposure. During exposure, a number of concentration gradients are set up. The PA distribution is aligned with the exposing fringe pattern; however, due to the absence of crosslinking agents in the material, the PA is not held so rigidly in place within the PVA matrix. AA and dye concentration gradients are also set up during exposure [25]. The dye molecule has a molecular weight of 373.9 u, which is much larger than that of AA, at 71.08 u [25]. It seems reasonable to assume that the AA, being the smaller molecule, will diffuse more rapidly to restore uniformity and will be largely responsible for any initial period of fast decay. The initial decay will also be contributed to by the diffusion of PA because it is both uncrosslinked and the layer is less viscous than it would become following longer exposures (i.e., dense polymerization).

Having made the assumption that the AA and shorter, less crosslinked PA chains are largely responsible for the period of fast decay, we now analyze the experimental results using Eq. (19) in Part I in order to extract a value for the diffusion associated with the grating modulation, D_M , postexposure. The value of D_M should approach that of D_{AA} from below as the exposure duration gets shorter. We again note that the PA will, in fact, have a distribution of molecular weights and diffusion rates. We neglect the effects associated with this in our analysis and assume that $D_{AA} \geq D_{PA} = \langle D_{PA} \rangle$.

3. DIFFUSION OF MATERIALS INTO AND OUT OF THE AA/PVA LAYER

In this section, we describe the diffusion of a compound across the boundaries into or out of the material layer. Subsection 3.A provides a brief introduction to diffusion between a layer and its surrounding environments. In Subsection 3.B, the mathematical theory used to determine the rate of diffusion is presented. Finally, in Subsections 3.C and 3.D, we describe the experimental methods used to find the rates of diffusion of water, propanol, and acetone, respectively, in our AA/PVA polymer layer.

A. Introduction to Diffusion in a Layer

Diffusion rates are affected by many factors, including temperature, pressure, solute size, and viscosity [26]. Increasing temperature brings the material closer to its glass transition temperature, T_g , and results in an increase in the rate of diffusion [27,28]. Decreasing the pressure can reduce binder density, thus increasing viscosity and making motion of the molecules less restricted. Similarly, the smaller the solute size, the easier it is to penetrate the film, resulting in a faster diffusion rate. Polar or charged particles may also interact more strongly with their surroundings [29], thus decreasing their mobility.

Polymer diffusion constants vary significantly due to their wide range of properties. However, in general, particle diffusion rates in polymer matrices should lie somewhere between those in crystalline solids and liquids [26]. The diffusion rates

are also known to have a strong dependence on concentration and the degree of swelling of the polymer layer [26]. We note that the material under study here is made up of a number of constituents, one of these being PVA, which has a $T_g \sim 70$ °C [30] and a high affinity for water (i.e., it is hydrophilic) [29].

In Subsection 2.B, we derived our model of PA diffusion, assuming that our process obeys Fick's first law. Let the amount of solvent absorbed per unit area of a polymer layer from its environment, at time t , M_t , be represented by [31]

$$M_t = k t^n, \quad (1)$$

where k is a constant and n is a parameter related to the diffusion mechanism, the value of which lies between 0.5 and 1. The case where $n = 0.5$ describes Fickian diffusion, and $n = 1$ describes type II diffusion [31]. These are limiting cases with anomalous diffusion taking place when $0.5 < n < 1$. Based on our experimental results (see Subsection 4.C), the observed diffusion of the materials examined into and out of the AA/PVA layer are Fickian and can reasonably be described by Fick's first law [31].

B. Theoretical Analysis of Diffusion into and out of a Layer

One surface of the polymer layer is in contact with a glass substrate while the other is exposed to the environment. The glass-polymer boundary is an impermeable surface and is treated as a zero concentration gradient. We assume that the layer is thin and, thus, that diffusion does not occur from the edges but rather in one dimension only, i.e., into the plane. This can be justified so long as $\ell/a \leq 0.02$, where ℓ is the layer thickness [31] and a is the shortest distance from the center of the layer to the edge. Assuming a maximum thickness of 250 μm , then with $a = 1.25$ cm, $\ell/a < 0.0196$. The smaller this ratio, the more accurate the model.

Next, consider diffusion into a polymer layer, bound by two parallel planes at $x = -\ell$ and $x = \ell$, both with constant concentration at the boundaries. In this case, there is symmetry about $x = 0$ and there is no diffusion across this central plane. As a result of this symmetry, the problem can be reduced to considering only half the layer, from $0 \leq x \leq \ell$. This corresponds to our case where one plane is bounded by an impermeable surface while the other is exposed to an environment where C , the concentration of the diffusing substance, is constant.

Given these conditions, we apply Fick's second law of diffusion,

$$\frac{\partial C}{\partial t} = D \frac{\partial^2 C}{\partial x^2}. \quad (2)$$

In Eq. (2), D is the diffusion coefficient of the diffusing material and is assumed to be constant throughout the medium layer and at all times during diffusion. Equation (2) is solved by using the Laplace transform to eliminate the time variable, reducing the problem to that of solving an ordinary differential equation. Following the derivation by Crank [31], this leads to

$$\frac{\partial^2 \bar{C}}{\partial x^2} - \frac{1}{D} \left[(C e^{-pt})_0^\infty + p \int_0^\infty C e^{-pt} dt \right] = 0, \quad (3)$$

where $\bar{C} = C_0/p$ and C_0 is the initial concentration of the diffusing substance within the layer. The boundary condition

Table 1. Initial and Boundary Conditions

	IC	BC1	BC2
Position condition	$0 \leq x \leq \ell$	$x = \ell$	$x = 0$
Concentration condition	$C = C_0$	$C = C_1$	$\partial C / \partial x = 0$
Time condition	$t = 0$	$t \geq 0$	$t \geq 0$
Resulting equation	$D \frac{\partial^2 \bar{C}}{\partial x^2} = p\bar{C} - C_0$	$\bar{C} = C_0/p$	$\partial \bar{C} / \partial x = 0$

(BC) and initial condition (IC) are summarized and applied as shown in Table 1. Following the analysis presented in [31], the solution for C can be written as a trigonometrical series to give the concentration equation as $t \rightarrow \infty$:

$$\frac{C - C_0}{C_1 - C_0} = 1 - \frac{4}{\pi} \sum_{n=0}^{\infty} \frac{(-1)^n}{2n+1} \exp\left\{\frac{-D(2n+1)^2\pi^2 t}{4l^2}\right\} \cos\frac{(2n+1)\pi x}{2l}, \quad (4)$$

where $n \in Z$ and C_1 is the concentration of the diffusing substance outside the layer. Then, if M_t is the total mass of diffusing substance, e.g., water, in the layer at time t , and M_∞ is the total mass diffusing in the layer after infinite time, we have [31]

$$\frac{M_t}{M_\infty} = 1 - \sum_{n=0}^{\infty} \frac{8}{(2n+1)^2\pi^2} \exp\left\{\frac{-D(2n+1)^2\pi^2 t}{4l^2}\right\}, \quad (5)$$

where M_t is given by

$$M_t = \int_0^l (C - C_0) dx. \quad (6)$$

To process the data obtained in the experiments described in Subsections 3.C and 3.D, we fit Eq. (5) to the results and determine the material diffusion coefficient, D , in the film.

C. Experimental Method to Find D

There are a number of experimental techniques available to determine the diffusion coefficient of a particular compound in a polymer film, including scanning IR microscopy, light scattering, neutron scattering, nuclear magnetic resonance, Raman scattering, IR spectroscopy, and ellipsometry [32–35]. Our experimental procedure is an established standard physical chemistry technique and gives an estimation of the diffusion rates in the material.

In all cases, the AA/PVA material under experiment was prepared as described in Subsection 2.A. The balance used for the mass measurements was a Sartorius Extend balance (model ED224S) [36] accurate to ± 0.05 mg.

In measuring the diffusion constant of water, the layers were stored in dessicators prior to measurement. Saturated salt solutions were used in the dessicators to maintain constant relative humidity (RH). Silica gel, potassium acetate solution, and sodium chloride solution were used to maintain the chambers at 12%, 25%, and 78% RH, respectively [37]. The humidity and temperature in the weighing chamber remained constant during the experiment, typically at 42% and 23 °C. Digital hygrometers/thermometers were used to constantly monitor the RHs and temperatures, with the tem-

perature during the course of the experiments ranging at most over 20–23 °C.

The experimental procedure was as follows. The polymer layer was exposed to a constant RH in a desiccation chamber for a period of time until it reached equilibrium with its surroundings. The layer was then rapidly transferred to the balance inside a sealed plexiglass chamber, which was maintained at a different RH but at the same temperature. The weight of the layer, RH, and temperature were monitored continuously and accurately with time until the samples reached equilibrium.

Under these conditions, any increase or decrease in the weight of the medium will arise due to water diffusing into, or out of, the layer from the surrounding environment and will be governed by Eq. (5). Experimental graphs of weight change as a function of time are fit using Eq. (5) to estimate values of the diffusion constant.

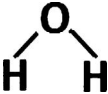
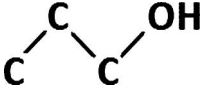
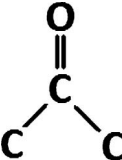
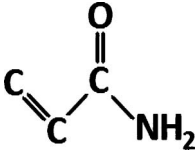
The procedure was carried out for both unpolymerized and uniformly photopolymerized layers, i.e., layers illuminated continuously using an extended exposure with a uniform beam. There were two aims in doing this: first, to compare the level of hydrophilicity of the layer both before and after the AA monomer has been completely polymerized [38]. If PA preferentially attracts water, greater swelling would take place in exposed areas. The second aim is to compare water diffusion rates into and out of polymerized and unpolymerized layers and determine if there was a significant change in the diffusion constant of the water. It was found that there was little difference in the results for diffusion of water into and out of the layer between polymerized and unpolymerized layers. This result is important, as a significant difference in diffusion between the two cases would impact on the material behavior postexposure. Exposed and unexposed regions would absorb significantly different amounts of water at different rates, which could lead to either a relative strengthening or weakening of the recorded pattern in the layer.

Carrying out this experiment for water provides a first estimate of an upper limit on the rate of diffusion of the AA monomer in the layer. Using the same procedure, results for two other materials, propanol and acetone, are also examined. In all three cases, the molecules used were smaller (lighter) than the AA molecules. While water has a relatively low molecular weight compared to AA, it is also highly polar, which influences the rate of diffusion of water in the layer. The propanol and acetone have molecular weights slightly lower than AA, but are significantly less polar than water. The polarity of a molecule is described by its dipole moment and its relative dielectric constant [39]. Table 2 presents values for both the molecular weights, melting and boiling points, radii, dipole moments, and the relative dielectric constant for water, AA, and the other materials used. We note that, in Table 2, no definitive dipole moment or molecular radius values for AA are presented because, to our knowledge, none are available in the literature [40,41].

D. Diffusion Rates of Propanol and Acetone in the Material

One hydrocarbon chosen as part of this study was propanol. Propanol was chosen because of its similarity in molecular weight and structure to AA. It is also of interest because, chemically, propanol can act as a chain transfer agent in

Table 2. Structure and Properties of Diffusing Chemicals

	Water	Propanol	Acetone	Acrylamide
Chemical formula	H ₂ O	C ₃ H ₈ O	C ₃ H ₆ O	C ₃ H ₅ O
Chemical structure				
Molecular weight (g/mol)	18 [48]	60.09 [48]	58.09 [48]	71.08 [48]
Melting point/boiling point, (°C)	0/100 [48]	-126.5/97.1 [48]	-94.9/56.3 [48]	84.5/125 [48]
Dielectric constant/dipole moment (D)	80.1/1.85 [49,50]	20.1/1.68 [51,52]	20.7/2.91 [52,53]	2.8/0.12-3.42 [40,41]
Molecular radius (Å)	2.78 [54]	6.19 [55]	~6 [56]	Not available, but ~7 [57] ^a

^aNo definitive value available for AA in the literature. Value estimated by summing over bond lengths.

the polymerization process of AA [42]. Experimentally, it is convenient because it is a vapor at room temperature and can readily diffuse into and out of the polymer layer. In order to avoid relying completely on results from a single hydrocarbon test material, acetone was chosen for similar reasons as a second suitable test material.

In both cases, the experimental procedure is similar to that used for water with the exception that, prior to weighing, the layer was placed in a secure temperature-controlled chamber with propanol (acetone), and then allowed to stand for a fixed period of time (~12 h). It was then removed from the propanol (acetone) atmosphere, placed on the scale, and the weight change was monitored. The diffusion constant of propanol (acetone) was then determined. We note that the concentration of water in the atmosphere both inside and outside the chamber was the same, and, as a result, there was no water gradient (i.e., the water concentration was in equilibrium and equal amounts diffused into and out of the layer). Therefore, the weight change in the layer after being in the presence of the hydrocarbon rose solely as a result of the hydrocarbon leaving the layer.

4. EXPERIMENTAL RESULTS

In Subsection 4.A, we present our holographic exposure-based results for the diffusion of PA in the photopolymer layer for long exposures, as described in Section 2, while in Subsection 4.B, we present the corresponding results for short exposures. Then, in Subsections 4.C and 4.D, we describe the weight-based results obtained for water and propanol (acetone), respectively. Finally, Subsection 4.E presents a brief overview of the experimental results.

A. Results for Diffusion of PA: Long Exposures

The results presented in this subsection refer to the determination of the rate of diffusion of the PA postexposure, following long exposures. Experiments were carried out using varying amounts of BA crosslinker (0.0, 0.2, 0.4, and 0.8 g/100 ml), and the rate of diffusion was estimated in each case.

As expected, inclusion of a crosslinker resulted in a reduction of the value of the diffusion coefficient, which depended on the quantity of BA in the AA/PVA layer. The absence of BA results in less constrained, more easily diffusing PA chains, with rates closer to, but slower than, the rate of diffusion of the AA.

For each concentration of BA, these experiments were repeated a number of times, and the results are summarized in Table 3. Applying the procedure described in Subsection 2.C and in Subsection 3.C in Part I, we extract n_M , and then plot $\ln[n_M(t) - n_M(t_{\text{final}})]$ versus time, resulting in Fig. 2. This graph illustrates the decay of the spatial distribution of the PA with respect to time. A different concentration of the crosslinker was used for each curve in the graph, further illustrating how the increase in the crosslinking agent results in increased stability of the grating. Values for α_M were determined from the slope of the graph, as in Subsection 2.C, and, hence, the diffusion coefficient is then found using Eq. (19) in Part I.

The resulting estimates for the diffusion coefficients are presented in Table 3. An estimation for D_{PA} in the material containing 0.8 g/100 ml of crosslinker is found to be of the order 10^{-15} cm²/s, which indicates high stability and is consistent with previous results by Gallego *et al.* and Blaya *et al.* [5,7]. The results obtained for a reduced concentration of BA agree with those reported by O'Neill *et al.* [19]. For the case where the material contains no crosslinker, the effective rate of diffusion of the PA is estimated to be $\sim 10^{-13}$ cm²/s. While, as noted, the layer contains a distribution of PA

Table 3. Synopsis of Experimental Results for Diffusion Coefficients

PA, D_{PA}	Average $D \pm \Delta D$, cm ² /s
With 0.8 g/100 ml BA crosslinker	$(7.77 \pm 4.47) \times 10^{-15}$
With 0.4 g/100 ml BA crosslinker	$(3.36 \pm 0.75) \times 10^{-14}$
With 0.2 g/100 ml BA crosslinker	$(8.41 \pm 2.68) \times 10^{-14}$
Without BA crosslinker	$(1.49 \pm 0.82) \times 10^{-13}$
Short-exposure diffusion rate (no BA crosslinker), D_{PA}	
1 s exposure	$(4.56 \pm 0.86) \times 10^{-11}$
3 s exposure	$(3.27 \pm 0.45) \times 10^{-11}$
6 s exposure	$(2.33 \pm 0.24) \times 10^{-11}$
9 s exposure	$(1.80 \pm 0.11) \times 10^{-11}$
Water (diffusion both in and out of the layer), D_W	
Thickness = 100 μ m	$(1.22 \pm 0.62) \times 10^{-8}$
Thickness = 220 μ m	$(5.90 \pm 3.00) \times 10^{-8}$
Propanol (diffusion out of the layer), D_{Prop}	
Thickness = 100 μ m	$(1.86 \pm 0.52) \times 10^{-8}$
Thickness = 220 μ m	$(9.00 \pm 2.52) \times 10^{-8}$
Acetone (diffusion out of the layer), D_{Ace}	
Thickness = 100 μ m	$(1.76 \pm 0.47) \times 10^{-8}$
Thickness = 220 μ m	$(8.52 \pm 2.27) \times 10^{-8}$

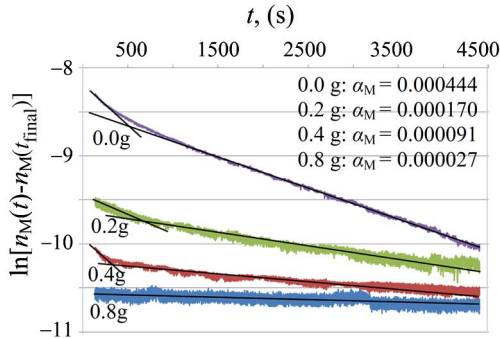


Fig. 2. (Color online) Grating decay over time for varying crosslinker quantities.

molecular weights, this value provides a convincing lower limit for the monomer diffusion constant.

Returning to Fig. 2, we note that a different and significantly higher rate of decay can be associated with the early parts, $t < 500$ s, of the postexposure curves. It seems reasonable to assume that diffusion by smaller, faster molecules is dominating the decay process. Therefore, these rates must be closer to that of the AA molecules. Thus, studying this behavior might prove useful in determining D_{AA} .

B. Results for Diffusion of PA: Short Exposures

Having examined our results for long exposures, we now examine the case of relatively short holographic illumination. In this case, much of the monomer present in the layer remains unpolymerized. The overall result of shortening the exposures, in terms of the expected diffusion rate associated with the decay of the grating modulation, will be that the diffusion process will be dominated by the AA molecules and the fewer, less entangled polymer chains, resulting in a diffusion rate closer to the rate of diffusion of monomer.

All the curves in Fig. 3 are for layers containing no crosslinker. As expected for short exposures, the diffraction efficiency observed is very low, indicating weak grating modulation. Also, as expected, the diffraction efficiency decays quickly. Using the same procedure as in Subsection 4.A, the grating decay curves were obtained, as seen in the inset in Fig. 3. Paying particular attention to the period of time immediately postexposure, the slope of the decay curve, α_M , is estimated. Using Eq. (19) in Part I, this value is then used to find the rate of diffusion of the grating modulation, D_M .

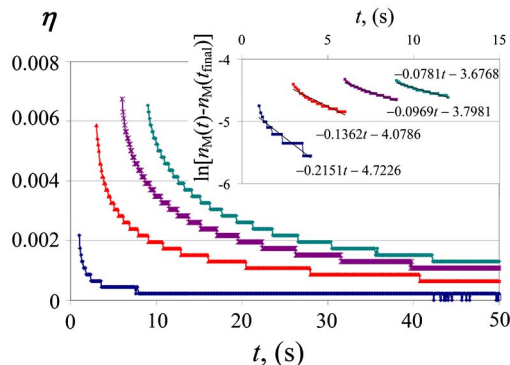


Fig. 3. (Color online) Short-exposure curves showing diffraction efficiency and corresponding grating decay curves (inset) for a range of exposure times when no crosslinking agent is present.

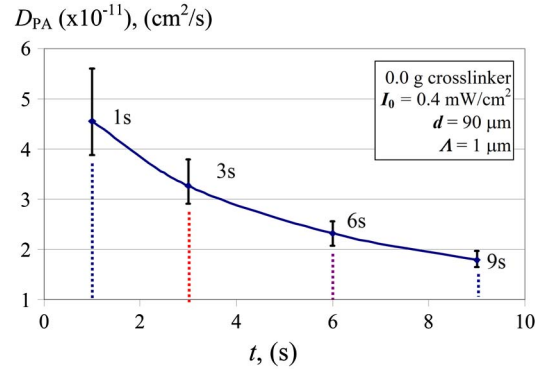


Fig. 4. (Color online) Curve showing diffusion rates for different exposure durations.

The results obtained are presented in Table 3 and illustrated in Fig. 4. The rates of diffusion estimated consistently decrease as the exposure duration increases. For the shortest exposure duration, the rate of diffusion of the grating modulation was found to be $D_M \approx (4.56 \pm 0.86) \times 10^{-11} \text{ cm}^2/\text{s}$. As previously discussed, we expect this value to approach that of D_{AA} from below. It should be noted, however, that continued grating growth postexposure is not taken into account in our analysis [45]. The effect of continued dark polymerization is to reduce the rate of decay, thus, the actual value of diffusion immediately postexposure may be slightly higher than that estimated here.

C. Diffusion of Water into and out of the Layer

We now present our weight-based experimental results and the estimated rate of diffusion of water, D_W , and then of various hydrocarbons (i.e., propanol, D_{Prop} , and acetone, D_{Ace}) in the AA/PVA layer. The weight change over time is used to estimate the diffusion coefficient of water into and out of the photopolymer layer using Eq. (5). The weights given in all the graphs are for the difference between the weight at a given time and the starting or initial value.

Figure 5 contains results for diffusion of water into and out of two typical layers plotted against the square root of time. The linear initial rise and subsequent flattening of the graph once equilibrium has been established supports our assumption that Fickian diffusion is taking place. Experiments were carried out for both the unpolymerized and polymerized layer, i.e., where the plates had been uniformly exposed to light and all the monomers had been polymerized. This was done to

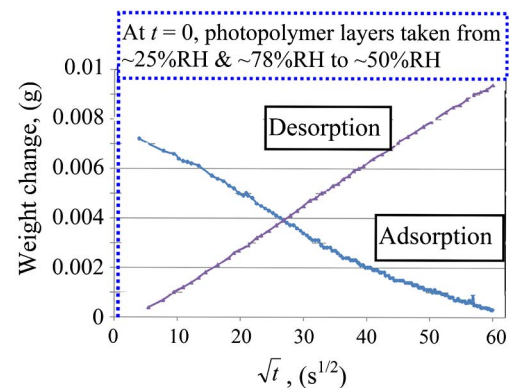


Fig. 5. (Color online) Weight change due to water plotted against the square root of time.

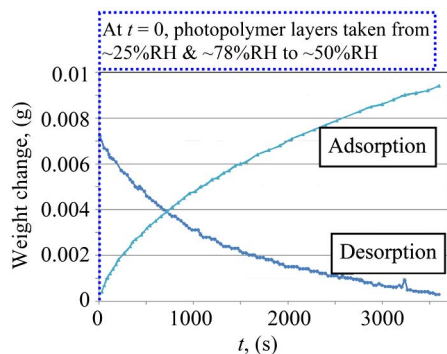


Fig. 6. (Color online) Weight change due to water gain/loss as a function of time.

determine whether there is an appreciable difference in the mobility of the small water molecule in the layer depending on the state of polymerization. As noted, there is a small difference between the diffusion rate of water in the unpolymerized and the polymerized material, with there appearing to be a consistent increase of $\sim 4\%$. However, this was within the limits imposed by experimental error and requires further verification using more sensitive techniques. We note that triethanolamine, the electron donor and radical initiator, is also hydrophilic, and makes up $\sim 49\%$ of the total volume of the layer [14,46].

To obtain Fig. 6, a layer, which had been stored in a desiccator, was placed on the weighing scales in a stable environment having a higher/lower humidity than the desiccator environment. This results in a change in the layer weight. In each case, the best fits to the experimental data were found. Figure 7 shows data from two experiments and the fits to this data using Eq. (6). In Fig. 7(b), the data displayed is for water diffusing into the layer as the material was transferred from a potassium acetate environment with an RH of $\sim 25\%$ into an environment having an RH of $\sim 50\%$, with the temperature remaining constant.

In Fig. 7(a), the results for D_W found for the case when water diffuses out of a layer is presented. In this case, the plate is first stored in a high-humidity environment, and is then placed on the weighing scale in a low-humidity environment. The material is transferred from an RH of $\sim 78\%$ to an RH of $\sim 50\%$, again with the temperature remaining constant. The weight decreases as expected, and fits to the experimental results are presented for different layer thicknesses. In all cases, diffusion constants of $\sim 10^{-8} \text{ cm}^2/\text{s}$ are estimated (see Table 3).

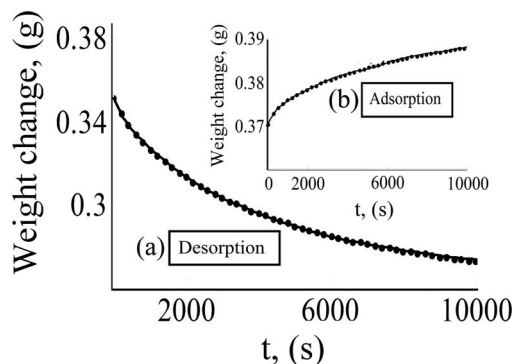


Fig. 7. Weight change over time for (a) water out and (b) water in. Experimental (dots) and theoretical results (curves).

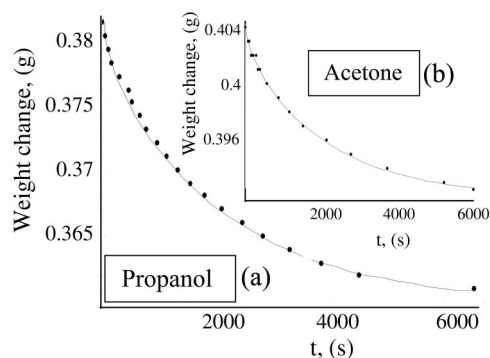


Fig. 8. Weight change over time for diffusion of (a) propanol and (b) acetone out of a layer. Experimental (dots) and theoretical results (curves).

D. Diffusion of Propanol and Acetone into the Layer

Similarly, the rates of diffusion of both propanol, D_{Prop} , and acetone, D_{Ace} , out of the polymer layer were determined. Because of the strong affinity of propanol (acetone) to the layer material, exposing the layer for several days resulted in the AA/PVA layer absorbing so much that the layers reliquified. Hence, the layers were only exposed to the propanol (acetone) environment for a maximum of 12 h. In this case, the transport of the hydrocarbon in the PVA layer takes place under a Fickian mechanism. Experimental data for the weight change as the propanol (acetone) exited the layer was then measured. The data was fit using Eq. (5), and diffusion rates for the propanol (acetone) were found.

In Fig. 8, theoretical and experimental results for the diffusion of (a) propanol and (b) acetone out of a layer are shown. For propanol, the value of D_{Prop} was found to be $\sim 10^{-8} \text{ cm}^2/\text{s}$. Similarly, for acetone, D_{Ace} was also found to be $\sim 10^{-8} \text{ cm}^2/\text{s}$.

The physical accuracy of the model of bulk diffusion into and out of the layer depends on the assumption that $l/a \leq 0.02$. Experiments were carried out on layers 100 and $220 \mu\text{m}$ thick, which correspond respectively to l/a values of 0.008 and 0.0176. The thinner the layer, the more accurately the model describes the result obtained. In all cases examined, and for each diffusing material, the thinner layers resulted in a slower estimated rates of diffusion $\sim 1.5 \times 10^{-8} \text{ cm}^2/\text{s}$. Our results appear to conclusively restrict the value of D_{AA} to below $\sim 6 \times 10^{-9} \text{ cm}^2/\text{s}$, the slowest result obtained for D_W .

E. General Comments on the Results

It would seem reasonable to assume that the water would more rapidly diffuse in the polymer layer than propanol given the fact that the water molecule is less than a third the weight of the propanol molecule (18 compared to 60 u). However, as seen from the results presented in Subsections 4.C and 4.D, the rates of diffusion are similar. This appears to be because the water molecule is highly polar compared to both the propanol and acetone molecules and therefore interacts more strongly with the material in the layer.

Table 3 provides a synopsis of the results for the rate of diffusion of PA, found holographically, and the rates of diffusion of water, propanol, and acetone in the layer.

5. CONCLUSIONS

The rates of diffusion of several materials in a layer of photo-sensitive AA/PVA photopolymer have been examined using holographic and analytic physical chemistry methods. Using long holographic exposures, the diffusion of PA was examined. We note that the result consistently estimated for uncrosslinked PA, i.e., $D_{AA} > D_{PA} \sim 10^{-13} \text{ cm}^2/\text{s}$, agrees with previously reported results. Then, short-exposure experiments were carried out on uncrosslinked material, which suggested that, in this case, a rate of diffusion of $D_M \sim 10^{-11} \text{ cm}^2/\text{s}$ governs grating modulation decay. Since PA cannot diffuse more quickly than AA, this result places a convincing lower bound on the rate of diffusion of AA, i.e., $D_{AA} > 10^{-11} \text{ cm}^2/\text{s}$.

The rates of diffusion of water, propanol, and acetone were also determined using a weight-based technique. The rates of diffusion of these three materials suggest an upper limit for the rate of diffusion of the AA monomer in the layer. The rates of diffusion D_W , D_{Prop} , and D_{Ace} were all found to be $\sim 10^{-8} \text{ cm}^2/\text{s}$ (see Table 3), with the slowest result (for the thinnest layers) being $D_W \sim 6 \times 10^{-9} \text{ cm}^2/\text{s}$. Given that AA has a larger molecular weight than all three, is a solid at room temperature, and is structurally bigger and more complex, it seems reasonable to expect that AA will diffuse more slowly, i.e., $D_{AA} < 6 \times 10^{-9} \text{ cm}^2/\text{s}$.

From Part I of this work, experimental upper estimates for $D_{AA} \sim 10^{-9} \text{ cm}^2/\text{s}$ were found. However, as indicated in Part I, this value is high because the optical effect of the surface relief gratings is not completely eliminated due to imperfect index matching during coverplating. The upper bound is therefore closer to $10^{-10} \text{ cm}^2/\text{s}$. We note that using the NPDD model values for D_{AA} of $\sim 10^{-11}$ – $10^{-10} \text{ cm}^2/\text{s}$ have been consistently estimated [14,47].

In summary, the fastest value of D_{PA} , i.e., for uncrosslinked materials and short exposures, provides a lower limit for the AA diffusion constant of $D_{AA} \sim 10^{-11} \text{ cm}^2/\text{s}$. Combining the weight-based results for water, propanol, and acetone and the results obtained in Part I gives an upper value of $D_{AA} \sim 10^{-10} \text{ cm}^2/\text{s}$. Therefore, a range of values, for the given range of temperatures, humidities, and exposures of material layers discussed, of $10^{-11} \sim D_{AA} \sim 10^{-10} \text{ cm}^2/\text{s}$ is indicated, and this result is consistent with the predictions of the NPDD model [14,47].

ACKNOWLEDGMENTS

We acknowledge the support of Enterprise Ireland, Science Foundation Ireland under the National Development Plan. We also acknowledge the support of the Irish Research Council for Science, Engineering and Technology.

REFERENCES

- C. E. Close, M. R. Gleeson, and J. T. Sheridan, "Monomer diffusion rates in photopolymer material. Part I. Low spatial frequency holographic gratings," *J. Opt. Soc. Am. B* **28**, 658–666 (2011).
- J. T. Sheridan, M. R. Gleeson, C. E. Close, and J. V. Kelly, "Optical response of photopolymer materials for holographic data storage applications," *J. Nanosci. Nanotech.* **7**, 232–242 (2007).
- I. Naydenova, R. Jallapuram, R. Howard, S. Martin, and V. Toal, "Investigation of the diffusion processes in a self-processing acrylamide-based photopolymer system," *Appl. Opt.* **43**, 2900–2905 (2004).
- T. Babeva, I. Naydenova, S. Martin, and V. Toal, "Method for characterization of diffusion properties of photopolymerisable systems," *Opt. Express* **16**, 8487–8497 (2008).
- S. Gallego, A. Marquez, D. Mendez, C. Neipp, M. Ortuno, A. Belendez, E. Fernandez, and I. Pascual, "Direct analysis of monomer diffusion times in polyvinyl/acrylamide materials," *Appl. Phys. Lett.* **92**, 073306 (2008).
- S. Gallego, A. Marquez, S. Marini, E. Fernandez, M. Ortuno, and I. Pascual, "In dark analysis of PVA/AA materials at very low spatial frequencies: phase modulation evolution and diffusion estimation," *Opt. Express* **17**, 18279–19291 (2009).
- S. Blaya, L. Carretero, P. Acebal, R. F. Madrigal, A. Murciano, M. Ulibarrena, and A. Fimia, "Analysis of the diffusion processes in dry photopolymerizable holographic recording materials," *Proc. SPIE* **5827**, 128–139 (2005).
- J. Ashley, M. P. Bernal, G. W. Burr, H. Coufal, H. Guenther, J. A. Hoffnagle, C. M. Jefferson, B. Marcus, R. M. MacFarlane, R. M. Shelby, and G. T. Sincerbox, "Holographic data storage technology," *IBM J. Res. Dev.* **44**, 341–368 (2000).
- F. T. O'Neill, A. J. Carr, S. M. Daniels, M. R. Gleeson, J. V. Kelly, J. R. Lawrence, and J. T. Sheridan, "Refractive elements produced in photopolymer layers," *J. Mater. Sci.* **40**, 4129–4132 (2005).
- G. P. Nordinand and A. R. Tanguay, Jr., "Photopolymer-based stratified volume holographic optical elements," *Opt. Lett.* **17**, 1709–1711 (1992).
- R. K. Kostuk, J. Castro, and D. Zhang, "Holographic low concentration ratio solar concentrators," in *Frontiers in Optics*, OSA Technical Digest (CD) (Optical Society of America, 2009), paper FMB3.
- J. Zhang, K. Kasala, A. Rewari, and K. Saravanamuttu, "Self-trapping of spatially and temporally incoherent white light in a photochemical medium," *J. Am. Chem. Soc.* **128**, 406–407 (2006).
- A. C. Sullivan, M. W. Grabowski, and R. R. McLeod, "Three-dimensional direct-write lithography into photopolymer," *Appl. Opt.* **46**, 295–301 (2007).
- J. V. Kelly, M. R. Gleeson, C. E. Close, F. T. O'Neill, J. T. Sheridan, S. Gallego, and C. Neipp, "Temporal analysis of grating formation in photopolymer using the nonlocal polymerisation-driven diffusion model," *Opt. Express* **13**, 6990–7004 (2005).
- M. R. Gleeson, J. V. Kelly, D. Sabol, C. E. Close, S. Lui, and J. T. Sheridan, "Modelling the photochemical effects present during holographic grating formation in photopolymer materials," *J. Appl. Phys.* **102**, 023108 (2007).
- S. Liu, M. R. Gleeson, J. Guo, and J. T. Sheridan, "High intensity response of photopolymer materials for holographic grating formation," *Macromolecules* **43**, 9462–9472 (2010).
- W. Kuhn and G. Balmer, "Crosslinking of single linear macromolecules," *J. Polym. Sci.* **57**, 311–319 (1962).
- S. Liu, M. R. Gleeson, and J. T. Sheridan, "Analysis of the photo-absorptive behaviour of two different photosensitisers in a photopolymer material," *J. Opt. Soc. Am. B* **26**, 528–536 (2009).
- F. T. O'Neill, J. R. Lawrence, and J. T. Sheridan, "Improvement of holographic recording material using aerosol sealant," *J. Opt. A Pure Appl. Opt.* **3**, 20–25 (2001).
- L. Aubrecht, M. Miller, and I. Koudela, "Recording of holographic diffraction gratings in photopolymers: theoretical modelling and real-time monitoring of grating growth," *J. Mod. Opt.* **45**, 1465–1477 (1998).
- H. Kogelnik, "Coupled wave theory for thick hologram gratings," *Bell Syst. Tech. J.* **48**, 2909–2947 (1969).
- C. E. Close, M. R. Gleeson, and J. T. Sheridan, "Using short exposures to approximate diffusion rates," *Proc. SPIE* **7717**, 771710 (2010).
- G. Zhao and P. Mouroulis, "Diffusion model of hologram formation in dry photopolymer materials," *J. Mod. Opt.* **41**, 1929–1939 (1994).
- S. Blaya, L. Carretero, R. F. Madrigal, M. Ulibarrena, P. Acebal, and A. Fimia, "Photopolymerization model for holographic gratings formation in photopolymers," *Appl. Phys. B* **77**, 639–662 (2003).
- J. Guo, S. Liu, M. R. Gleeson, and J. T. Sheridan, "Theoretical analysis and experimental validation of photosensitizer

- diffusion in a photopolymer material," *Proc. SPIE* **7717**, 77170Y (2010).
26. L. Masaro and X. X. Zhu, "Physical models of diffusion for polymer solutions, gels and solids," *Prog. Polym. Sci.* **24**, 731–775 (1999).
 27. O. Chiantore, L. Costa, and M. Guaita, "Glass temperatures of acrylamide polymers," *Macromol. Rapid Commun.* **3**, 303–309 (1982).
 28. A. V. Veniaminov and H. Sillescu, "Polymer and dye probe diffusion in poly(methyl methacrylate) below the glass transition studied by forced Rayleigh scattering," *Macromolecules* **32**, 1828–1837 (1999).
 29. W. M. Lee, "Selection of barrier materials from molecular structure," *Polym. Eng. Sci.* **20**, 65–69 (1980).
 30. S. Blaya, L. Carretero, P. Acebal, R. F. Madrigal, A. Murciano, M. Ulibarrena, and A. Fimia, "Analysis of the diffusion processes in dry photopolymerizable holographic recording materials," *Proc. SPIE* **5827**, 128–139 (2005).
 31. J. Crank, *The Mathematics of Diffusion*, 2nd ed. (Oxford University, 1975).
 32. J. S. Papanu, D. W. Hess, A. T. Bell, and D. S. Soane, "In situ ellipsometry to monitor swelling and dissolution of thin polymer films," *J. Electrochem. Soc.* **136**, 1195–1200 (1989).
 33. D. G. Bucknall, S. A. Butler, and J. S. Higgins, "Real-time measurement of polymer diffusion coefficients using neutron reflection," *Macromolecules* **32**, 5453–5456 (1999).
 34. E. D. Von Meerwall, "Self-diffusion in polymer systems measured with field-gradient spin echo NMR methods," in *Spectroscopy: NMR, Fluorescence, FT-IR*, H. Cantow, G. Dall'Asta, K. Dusek, J. D. Ferry, H. Fujita, M. Gordon, G. Henrici-Olivé, H. Kausch, J. P. Kennedy, W. Kern, S. Okamura, S. Olivé, C. G. Overberger, T. Saegusa, G. V. Schulz, W. P. Slichter, and J. K. Stille, eds. (Springer-Verlag, 1984), pp. 1–29.
 35. B. A. Westin, A. Axelsson, and G. Zacchi, "Diffusion measurement in gels," *J. Control. Release* **30**, 189–199 (1994).
 36. Sartorius Mechnronics, "Analytical balances ED," <http://www.sartorius-mechtronics.com/WW/en/Analytical-Balances/Analytical-Balances-ED-5iuzdcox3vk/a7pet8rq68/mp.htm?view=desc>.
 37. Omega Engineering, Inc., "Technical reference section," <http://www.omega.com/temperature/Z/zsection.asp>.
 38. S. Shukla, A. K. Bajpai, and E. A. Kilkarni, "Preparation, characterisation, and water-sorption study of polyvinyl alcohol based hydrogels with grafted hydrophilic and hydrophobic segments," *J. Appl. Polym. Sci.* **95**, 1129–1142 (2005).
 39. C. P. Smyth, *Dielectric Behaviour and Structure* (McGraw-Hill, 1955).
 40. Chemical Engineering Research Information Center, "Pure component properties," <http://www.chemic.org/research/kdb/>.
 41. I. M. El-Anwar, O. M. El-Nabaway, S. A. El-Hennwii, and A. H. Salama, "Dielectric properties of polyacrylamide and its utilization as a hydrogel," *Chaos Solitons Fractals* **11**, 1303–1311 (2000).
 42. M. J. Fevola, R. D. Hester, and C. L. McCormick, "Molecular weight control of poly (acrylamide) with sodium formate as a chain-transfer agent: characterization via size exclusion chromatography/multi-angle laser light scattering and determination of chain-transfer constant," *J. Polym. Sci., Part A: Polym. Chem.* **41**, 560–568 (2003).
 43. S. Gallego, A. Marquez, D. Mendez, C. Neipp, M. Ortuno, A. Belendez, E. Fernandez, and I. Pascual, "Direct analysis of monomer diffusion times in polyvinyl/acrylamide materials," *Appl. Phys. Lett.* **92**, 073306 (2008).
 44. S. Blaya, L. Carretero, P. Acebal, R. F. Madrigal, A. Murciano, M. Ulibarrena, and A. Fimia, "Analysis of the diffusion processes in dry photopolymerizable holographic recording materials," *Proc. SPIE* **5827**, 128–139 (2005).
 45. J. V. Kelly, M. R. Gleeson, C. E. Close, F. T. O'Neill, and J. T. Sheridan, "Temporal response and first order volume changes during grating formation in photopolymers," *J. Appl. Phys.* **99**, 113105 (2006).
 46. B. Cuq, N. Gontard, J. Cuq, and S. Guilbert, "Selected functional properties of fish myofibrillar protein-based films as affected by hydrophilic plasticizers," *J. Agric. Food Chem.* **45**, 622–626 (1997).
 47. M. R. Gleeson, D. Sabol, S. Liu, C. E. Close, J. V. Kelly, and J. T. Sheridan, "Improvement of the spatial frequency response of photopolymers by modifying polymer chain length," *J. Opt. Soc. Am. B* **25**, 396–406 (2008).
 48. Sigma Aldrich, "Solvent centre," www.sigmaldrich.com.
 49. M. Uematsu and E. U. Franck, "Static dielectric constant of water and steam," *J. Phys. Chem. Ref. Data* **9**, 1291–1306 (1980).
 50. S. A. Clough, Y. Beers, G. P. Klein, and L. S. Rothman, "Dipole moment of water from Stark measurements of H₂O, HDO and D₂O," *J. Chem. Phys.* **59**, 2254–2259 (1973).
 51. P. W. Khirade, A. Chaudhari, J. B. Shinde, S. N. Helambe, and S. C. Mehrotra, "Temperature dependant dielectric relaxation of 2-ethoxyethanol, ethanol, and 1-propanol in dimethylformamide solution using the time domain technique," *J. Solution Chem.* **28**, 1031–1043 (1999).
 52. L. Pogliani, "Model with dual indices and complete graphs. The heterogeneous description of the dipole moments and polarizabilities," *New J. Chem.* **27**, 919–927 (2003).
 53. R. S. Becker and K. Freedman, "A comprehensive investigation of the mechanism and photophysics of isomerisation of a protonated and unprotonated Schiff base of 11-cis-retinal," *J. Am. Chem. Soc.* **107**, 1477–1485 (1985).
 54. P. Kumar, F. W. Starr, S. V. Buldyrev, and H. E. Stanley, "Effect of water-wall interaction potential on the properties of nanoconfined water," *Phys. Rev. E* **75**, 011202 (2007).
 55. A. P. D'Silva, G. Harrison, A. R. Horrocks, and D. Rhodes, "Investigation into cotton fibre morphology part III: Effect of alcohol treatment on water absorption," *J. Text. Inst.* **91**, 123–131 (2000).
 56. R. E. Rebbert and P. Ausloos, "Quenching of the triplet state of acetone and biacetyl by various unsaturated hydrocarbons," *J. Am. Chem. Soc.* **87**, 5569–5572 (1965).
 57. F. H. Allen, O. Kennard, D. G. Watson, L. Brammer, A. G. Orpen, and R. Taylor, "Table of bond lengths determined by X-ray and neutron diffraction. Part 1. Bond lengths in organic compounds," *J. Chem. Soc. Perkin Trans. 2* **2**, S1–S19 (1987).